Thin films thermoelectric micro-devices for power generator applications using thermal evaporation method

A. HMOOD[*a,b], A. KADHIM[a,b], H. ABU HASSAN[a]
[a]*Nano-Optoelectronic Research and Technology Laboratory (N.O.R.), School of Physics, Universiti Sains Malaysia, 11800 USM, Penang, Malaysia*
[b]*Department of Physics, College of Science, University of Basrah, Basrah, Iraq*

In the current work p-$Pb_{0.94}Yb_{0.06}Se$:Se and n-$Pb_{0.94}Yb_{0.06}Se$ thin films were fabricated in a thermoelectric devices are composed of 20-pair and 10-pair deposited on a glass substrate using simple thermal evaporation method. The dimension of thin films thermoelectric micro-devices which consist of 20-pairs and 10-pair of legs connected by aluminum electrodes (Al-electrode) was 23 mm ×20 mm and 12 mm ×10 mm, respectively. The 20-pair p–n thermocouples in series device generated output maximum open-circuit voltage of 137.84 mV and a maximum output power up to 25.85 nW at temperature difference ΔT = 115 K, and 84.18 mV and 12.21 nW at ΔT = 162 K, for 10-pair, respectively at ΔT=128 K.

(Received September 3, 2012; accepted February 20, 2013)

Keywords: Thin films, Thermal evaporation method, Thermoelectronics, Thermoelectric generators

1. Introduction

Recently, the improvements in thermoelectric (TE) thin films have strongly increased in over a wide temperature range have spurred interest in micro-scale TE generators [1]. Although these TE thin films devices produced few micro-watts of power at relatively high-voltage there have been several applications calling for the operation of small electric devices and systems in the microelectronics industry [2, 3]. Micro thermoelectric generators can be used as a power source of small electronic devices, wireless sensors, and wearable electronics [4]. These include equipment used in military, aero space, medical, industrial, and consumer and scientific institutions [2, 5]. However, recent significant advances in the scientific understanding of quantum well and nanostructure effects on TE properties and modern thin layer and nano-scale manufacturing technologies have combined to create the opportunity of advanced TE materials with potential conversion efficiencies of over 15% [6]. The advent of these advanced TE materials offers new opportunities to recover waste heat more efficiently and economically with highly reliable and relatively passive systems that produce no noise and vibration[7, 8]. In the same time, the interest in producing micro-thermoelectric devices opens new opportunity in the field of micro power generation. Micro thermoelectric converters are a promising technology due to the high reliability, quiet operation and are usually environmentally friendly [9]. Recent developments in micro-thermoelectric devices using thin film deposition different growth methods based on MBE [10], MOCVD [11], RF co-sputtering [5, 12], a simple vacuum thermal evaporation [6], flash evaporation [2], and co-evaporation [4] have been used to grow single layers and super-lattices on various substrates [2] have shown that energy scavenged from human environment. TE generation have primarily focused on increasing the material figure of merit (ZT), which is the standard measure of a material's TE performance, and defined as $ZT = S^2\sigma T/\kappa$, where S is the Seebeck coefficient, σ the electrical conductivity, κ the thermal conductivity, and T is the absolute temperature. The product $S^2\sigma$ is defined as the thermoelectric power factor [13]. The power factor should be maximized and the thermal conductivity should be minimized in order to achieve high efficiency thermoelectric materials. In present study, we focus on the characterized and enhance micro-fabrication methods to improve the performance and integration of micro-scale TE generators. We prepare $Pb_{0.94}Yb_{0.06}Se$:Se as p-type ingot and $Pb_{0.94}Yb_{0.06}Se$ as n-type ingot for the fabrication 20-pair and 10-pair thermoelectric micro-devices (23 mm × 20 mm and 12 mm × 10 mm, respectively) of the thin films by a thermal evaporation method deposited onto glass substrates. First, investigate the intrinsic properties of each of the constituent thin films, and then we measure the output voltage and estimate the maximum output power of a complete generator near room temperature as functions of the temperature difference between hot and cold junctions.

2. Experimental

The n-type $Pb_{0.94}Yb_{0.06}Se$ was synthesized as a ternary compound by solid-state microwave standard. Weighted 2 g amounts, according to the stoichiometric ratio (1-x) : x : 1, were prepared from three high-purity element powders (Pb, Se ≥99.999% 100 meshes, and Yb ≥99.9% 157 μm) as described elsewhere [14]. The polycrystalline alloys of p-type of $Pb_{0.94}Yb_{0.06}Se$:Se prepared in above technique after added excess selenium element. The thin film thermoelectric generators are deposited onto clean glass substrates by thermal evaporation of 10^{-6} mbar at 300 K using silicon monoxide source design (SM) SO-20 series by (R. D. Mathis Co. USA). The p-type ($Pb_{0.94}Yb_{0.06}Se$:Se) and n-type ($Pb_{0.94}Yb_{0.06}Se$) powder is positioned in the boat in load cavity, when heated it follows an indirect path through a series of baffles and then out the vertical chimney, which the height's and diameter were 12 mm and 6.3 mm, respectively. So the substrates cannot see the bulk $Pb_{1-x}Yb_xSe$ material at any time, this, essentially, eliminates any chance of spitting and streaming, which causes pinholes. The distance between the tantalum bout and the substrate is 180 mm. The thicknesses of the thin films were determined to be approximately 0.947 µm using an optical reflectometer (Filmatric F20, USA) measurement system. The patterned shadow masks fabricated 20-pair and 10-pair thermoelectric micro-devices (23 mm×20 mm and 12 mm×10 mm, respectively) for the p and n-legs thin films and their junctions. Tracks on square substrates had 400 µm in width and 20 mm in length, on rectangular ones – 400 µm and 10 mm, respectively. The dimension of p- and n-legs was 20 mm (l) × 400 µm (w) × 0.947 µm (t), and the spacing between both legs was arranged to be 150 µm are shown in Fig. 1(a). A diffusion barrier layer (Al-electrode) was also deposited between p- and n-type of the thin film thermoelectric generator at the junctions. The fundamental physical parameters of semi-magnetic semiconductor lead chalcogenide thin films such as lattice constant, electrical conductivity, and the Seebeck coefficient are referred to in our previous papers [14]. We first measure the output voltage of the thin film thermoelectric generators while imposing a temperature gradients $\Delta T = T_h - T_c$ between hot and cold junctions of the generators. The schematic diagram of the measurement for the output voltage is shown in Fig. 1(b).

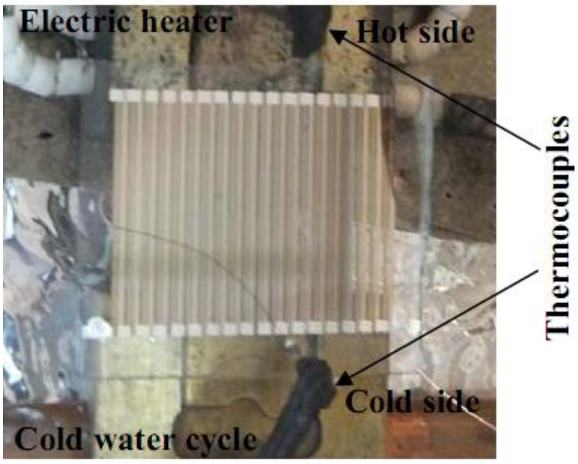

Fig. 1. (a) Photograph of 20-pair thin-film thermoelectric generator setup of the measurement of the output voltage (V_{out})

The output voltage V_{out}, and the respective current, I_{out} are measured at the silver paint pads connected to the thermoelectric legs. Measurement pairs of the voltage and current, $\{V_{out}, I_{out}\}$, are acquired while the load resistance, R_{load}, is manually adjusted. We also measure the overall resistance of the thin film thermoelectric generators by a two-wire method. The internal resistance, R_{in}, of the thermoelectric generator is calculated as follows: $R_{in} = V_{oc}/I_{sc}$, where Voc is the open-circuit voltage and I_{sc} is the short-circuit current. The maximum output power of the thin film thermoelectric generators is estimated from the output voltage and the overall resistance of the generators.

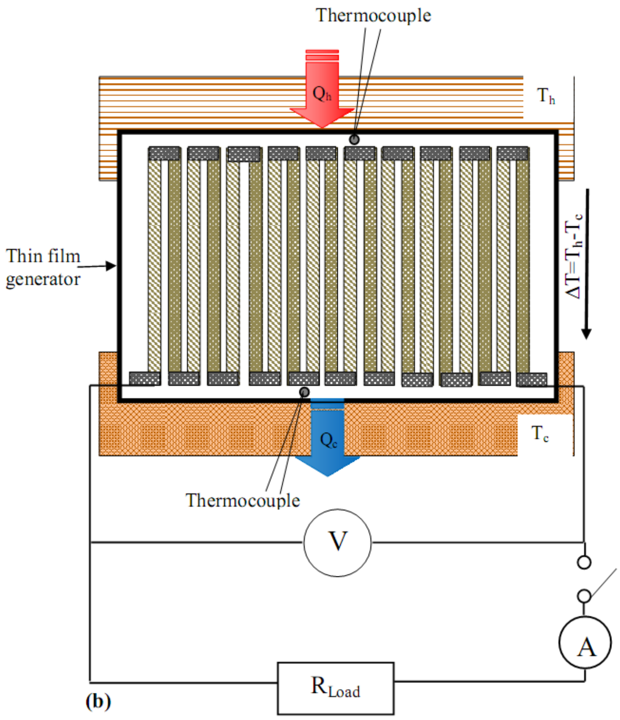

Fig. 1. (b) The schematic of the V_{oc} of the thin-film thermoelectric generators measured as functions of the temperature difference between the hot and cold junctions.

3. Results and dissection

The performance of lead–ytterbium−selenide-based micro-generators is investigated at temperature range of 298-460 K. Thus, a temperature difference ΔT was induced between hot and cold junctions of the micro-generators. The first set of tests consisted in the measurement the output voltage versus the output current output characteristic of the thermoelectric converter, and estimates the maximum output power. Fig. 2 shows the load characteristics of the two micro-generators, namely, the output voltage V_{out} versus the output current I_{out} as functions of the temperature difference ΔT for (a) 20-pair and (b) 10-pair micro-generators. As expected the output voltage increases with the temperature gradient, ΔT increased, and this conclusion is valid for the plot of the Fig. 2 and for similar plots, since the gradient temperatures are such that the thermoelectric converter is not behind a certain thermal saturation point. It can be observed a high linearity in all V_{out} v.s I_{out} plots and almost the same slope. This means that the internal resistance $R_{in} = V_{oc}/I_{sc}$ of the thermoelectric converter still constant with the gradient temperature and load resistance. From this analysis, it possible to conclude that the internal resistance of the analyzed thermoelectric device is equal to R_{in} = 183.78 KΩ for 20-pair, and 145.12 KΩ for 10-pair, respectively. An analysis to both plots of the Fig. 2 (a) and (b) allows the observation of an increasing in the output power, P_{out}, with the temperatures gradient.

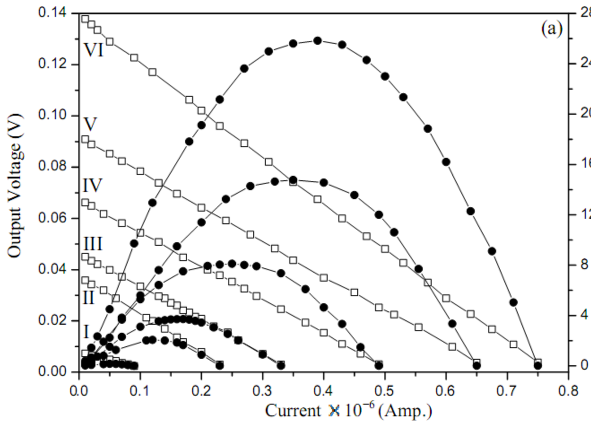

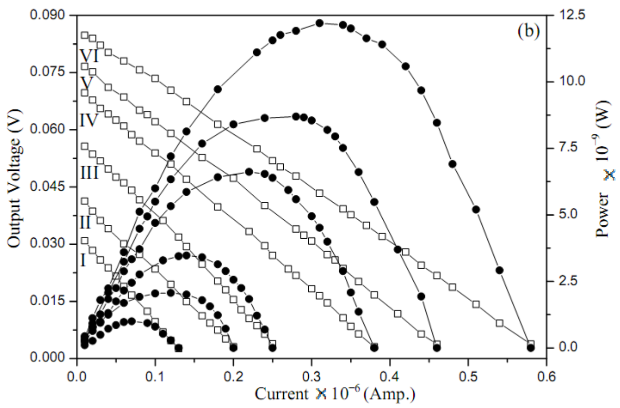

Fig. 2. Output power of the generators versus the output voltage (V_{out}) and output current (I_{out}) of (a) 20 pairs $Pb_{1-x}Yb_xSe$ micro-devices with different temperature gradients ΔT: (I) ΔT=15 K; (II) ΔT=32 K; (III) ΔT=47 K; (IV) ΔT=64 K; (V) ΔT=94 K; and (VI) ΔT=115 K. and (b) 10 pairs with different temperature gradients ΔT: (I) ΔT=27 K; (II) ΔT=42 K; (III) ΔT =57 K; (IV) ΔT=72 K; (V) ΔT=106 K; and (VI) ΔT=128 K.

Thus, the observation results from the rise of the temperature gradient, ΔT, whose consequence is an increase in the output voltage, V_{out}. As high is this output voltage, the high will be the output current I_{out} (considering several values for the load resistance) and therefore will be the dissipated power in the external load resistance, e.g. $P_{out} = R_{Load}I_{out}^2$. The alternative set of plots the output power, P_{out}, versus the output current, I_{out} (or versus the load resistance, R_{Load}). Fig. 2 illustrates six plots for the six difference temperatures, an alternative set of plots, but for the output power, Pout, versus the output voltage, Vout. The voltage, or thermoelectric electromotive force (emf), produced by Seebeck effect is defined as $V_{out} = S_{ab}\Delta T$, where S_{ab} indicates the relative Seebeck coefficient for the material pair a–b [9]. In order to maximize the generated output voltage, several thermocouples are connected electrically in series each other and thermally in parallel to form a thermopile, which is able to generate n times the output voltage of one thermocouple (if n is the number of thermocouples in series) and a maximum output electric power (with optimal impedance matching) can be expressed as $P_{max} = (nS_{ab}\Delta T)^2/4R_{in}$, where R_{in} internal electrical resistance of generator, the internal electrical resistance is calculated from their dimensions, the number of thermocouples in series, and the electrical resistance [15, 16]. Assuming that the maximum output power is achieved when $R_{Load} = R_{in}$, so the maximum output power of micro-generators estimated as functions of the temperature difference in this measured temperature region [15]. At the temperature difference of 115 K, the output voltage reaches 137.84 mV and 25.85 nW, respectively, for 20-pairs and 84.18 mV and 12.21 nW, respectively for 10-paris at 128 K. In fact, the thermoelectric generators are generally based on heavily doped semiconductors use the Seebeck effect to produce electrical energy [14-18]. In a thermoelectric generator, another performance factor is more appropriate, which is the power factor, $S^2\sigma$ ($W/K^2\ m^{-1}$). The $S^2\sigma$ is defined as the electric power per unit of area through which the heat flows, per unit of temperature gradient between the hot and the cold sides [19]. This is attributed to the structure not having been optimized and to the high contact resistance caused by the non-optimized bonding process [11]. It is well known that the electrical contact and thermal contact will play important roles in improving the device power-generation performance and need to be minimized.

4. Conclusion

Lead−ytterbium–selenide-based micro-generators are successfully fabricated by a thermal evaporation method, and their performance is improved by micro scale design. We measure the performance of the micro-generators at 298-460 K. The high output voltage of 137.84 mV, 84.18 mV and estimated output power of 25.85 nW, 12.21 nW for 20-pair and 10-pair, respectively, are obtained from a temperature difference ΔT = 115 and 128 K. Seebeck voltage and electrical power have shown a high voltage and low power generate for each device geometry. These maximum P_{out} of the thin film thermoelectric generators in this work is still not enough to apply as a power source for microelectronic devices. However, in the future opportunity to fabricate a higher output voltage device and output requirements will be obtained with about 100 thermocouples in series, and high an estimated output power with low temperature gradient.

Acknowledgment

The authors would like to the Nano-Optoelectronics Research and Technology Laboratory (N.O.R.) of the School of Physics for the help extended during the research. This work was supported by the Postgraduate Research Grant Scheme (PRGS) 1001/PFIZIK/844134 of the Universiti Sains Malaysia.

References

[1] M. Takashiri, T. Shirakawa, K. Miyazaki, H. Tsukamoto, Sens. Actuators A **138**, 329 (2007).
[2] G. Savelli, M. Plissonnier, J. Bablet, C. Salvi, J. M. Fournier, MEMS/MOEMS - DTIP (2006) ISBN: 2-916187-03-0.
[3] Il-Ho Kim, Mater. Lett. **43**, 221 (2000).
[4] Nam-Ho Bae, Seungwoo Han, Kwang Eun Lee, Byeongil Kim, Seon-Tai Kim, Current Appl. Phys. **11**, S40 (2011).
[5] N. Kaiwa, M. Hoshino, T. Yaginuma, R. Izaki, S. Yamaguchi, A. Yamamoto, Thin Solid Films **515**, 4501 (2007).
[6] M. Tan, Y. Wang, Y. Deng, Z. Zhang, B. Luo, J. Yang, Y. Xu, Sens. Actuators A **171**, 252 (2011).
[7] X. Niu, J. Yu, S. Wang, J. Power Sou. **188**, 621 (2009).
[8] D. Zhao, C. Tian, S. Tang, Y. Liu, L. Jiang, L. Chen, Mater. Sci. Semicond. Process. **13**, 221 (2010).
[9] L. Francioso, C. De Pascali, I. Farella, C. Martucci, P. Cretì, P. Siciliano, A. Perrone, J. Power Sou. **196**, 3239 (2011).
[10] G. Zeng, J-H Bahk, J. E. Bowers, H. Lu, A. C. Gossard, S. L. Singer, A. Majumdar, Z. Bian, M. Zebarjadi, A. Shakouri, Appl. Phys. Lett. **95**, 083503 (2009).
[11] S. D. Kwon, B. K. Ju, S. J. Yoon, J. S. Kim, J. Electron. Mater. **38**(7), 920 (2009).
[12] R. Izaki, M. Hoshino, T. Yaginuma, N. Kaiwa, S. Yamaguchi, A. Yamamoto, Microelectronics Journal **38**, 667 (2007).
[13] A. Hmood, A. Kadhim, H. Abu Hassan, Superl. Microst. **53**, 39 (2013).
[14] A. Hmood, A. Kadhim, H. Abu Hassan, J. Alloys Compd. **520**, 1 (2012).
[15] Y. Pei, A. D. La Londe, S. Iwanaga, G. J. Snyder, Energy Environ. Sci. **4**, 2085 (2011).
[16] Yu. I. Ravich, S. A. Nemov, Semiconductors **36**, 1 (2002).
[17] H. S. Dow, M. W. Oh, B. S. Kim, S. D. Park, B. K. Min, H. W. Lee, D. M. Weel, J. Appl. Phys. **108**, 113709 (2010).
[18] H. Wang, Y. Pei, A. D. LaLonde, G. J. Snyder, Adv. Mater. **23**, 1366 (2011).
[19] J. P. Carmo, Joaquim Antunes, M. F. Silva, J. F. Ribeiro, L. M. Goncalves, J. H. Correia, Measurement **44**, 2194 (2011).

*Corresponding author: arshad.phy73@gmail.com